AGU PUBLICATIONS

Geophysical Research Letters

RESEARCH LETTER
10.1002/2017GL076489

Key Points:
- New flow power sediment entrainment model scales with flow depth instead of particle size and incorporates capacity and competence limits
- Suspended load, at the threshold between net erosion and deposition, is shown to be controlled by the particle size distribution
- Flow power model offers an order of magnitude, or better, improvement in predicting the erosional-depositional threshold

Supporting Information:
- Table S1
- Supporting Information SI

Correspondence to:
R. M. Dorrell,
r.dorrell@hull.ac.uk

Citation:
Dorrell, R. M., Amy, L. A., Peakall, J., & McCaffrey, W. D. (2018). Particle size distribution controls the threshold between net sediment erosion and deposition in suspended load dominated flows. *Geophysical Research Letters*, *45*, 1443–1452. https://doi.org/10.1002/2017GL076489

Received 28 NOV 2017
Accepted 23 JAN 2018
Accepted article online 29 JAN 2018
Published online 15 FEB 2018

Particle Size Distribution Controls the Threshold Between Net Sediment Erosion and Deposition in Suspended Load Dominated Flows

R. M. Dorrell[1], L. A. Amy[2], J. Peakall[3], and W. D. McCaffrey[3]

[1]Energy and Environment Institute, University of Hull, Hull, UK, [2]School of Earth Sciences, University College Dublin, Dublin, Ireland, [3]School of Earth and Environment, University of Leeds, Leeds, UK

Abstract The central problem of describing most environmental and industrial flows is predicting when material is entrained into, or deposited from, suspension. The threshold between erosional and depositional flow has previously been modeled in terms of the volumetric amount of material transported in suspension. Here a new model of the threshold is proposed, which incorporates (i) volumetric and particle size limits on a flow's ability to transport material in suspension, (ii) particle size distribution effects, and (iii) a new particle entrainment function, where erosion is defined in terms of the power used to lift mass from the bed. While current suspended load transport models commonly use a single characteristic particle size, the model developed herein demonstrates that particle size distribution is a critical control on the threshold between erosional and depositional flow. The new model offers an order of magnitude, or better, improvement in predicting the erosional-depositional threshold and significantly outperforms existing particle-laden flow models.

1. Introduction

When particle-laden flows erode or deposit material, the fundamental properties of the flow (hydrodynamics), and through time, the surfaces over which a flow travels (morphodynamics) are changed. Therefore, whether a flow is net erosional or depositional is of key importance in environmental and industrial fluid dynamics, for example, on landscape erosion and evolution (Bufe et al., 2016; Houssais et al., 2015), the efficiency of hydraulic engineering structures such as dams (Wang et al., 2015; Yang, 2006), the effectiveness of flood protection measures (Nittrouer et al., 2012), and pipe flow obstruction or erosion-corrosion (Parsi et al., 2014). Equivalent terminology may use subsaturated flow and supersaturated flow to define if a flow is net erosional or depositional (van Maren et al., 2009). The threshold between erosion and deposition, that is, the condition of equilibrium in particle-laden flow, is arguably the most important prediction a sediment transport model is required to make. Hence, here we use the prediction of the threshold between net erosional and net depositional flow, as the key criterion for testing sediment transport models.

In natural flows, sediments are predominately transported by turbulent fluid motion as suspended load, and material interacting with the bed (bedload) is negligible in terms of bulk sediment flux (Syvitski et al., 2003); consequently, we concentrate on modeling the transport of suspended load. In keeping with most existing predictions of suspended load transport, we assume low concentration, non-cohesive sediment suspensions, and model the limiting threshold where sediment erosion balances deposition (Yang, 2006). Therefore, in dilute flow, sediment concentration below or above an equilibrium value respectively defines if a flow is net erosional or depositional (van Maren et al., 2009). The test of the suspended load transport models is thus the comparison of observed versus predicted hydrodynamic and suspended load conditions at the net erosion-deposition threshold.

Common suspended load transport models are based on flow velocity, depth, concentration, and a single characteristic particle size (i.e., monodisperse models; Bagnold, 1966; Bizzi & Lerner, 2015; Celik & Rodi, 1991; Garcia, 2008; Kubo et al., 2005; Velikanov, 1954; Yang, 2006), often the median particle diameter. Although suspended load transport models can show good agreement with individual sets of laboratory or field-based observations, they invariably show poorer agreement when compared with other empirical data sets (Walling, 2009; Yang, 2006). However, the particle size distribution of sediment in natural (Bayat et al., 2015) and industrial flows (Parsi et al., 2014; Sajeesh & Sen, 2014) is often wide and fine-tail skewed (motivating the standard use of a log-normal particle size scale; Garcia, 2008; Soulsby, 1997). As has been

previously recognized, particle distribution may affect sediment transport processes (Smith & Hopkins, 1973); thus, some numerical sediment transport models use finite discretization of particle size distributions, that is, polydisperse models, to simulate the transport dynamics of particles of mixed sizes (Armanini & Di Silvio, 1988; Basani et al., 2014; Blom & Parker, 2004; Dorrell, Hogg, & Pritchard, 2013; Garcia & Parker, 1991; Halsey et al., 2017; McLean, 1991, 1992; Strauss & Glinsky, 2012; Wilcock & Southard, 1988). However, the effect of mixed size distributions, that is, polydispersity, on the threshold between erosion and deposition from suspended load particle transport, and thus the effectiveness of common monodisperse models of sediment transport at the deposition-erosion threshold, has not been robustly investigated.

A further key shortcoming of most sediment transport models is that capacity and competence are not jointly considered. Capacity describes the maximum amount of material that a turbulent flow can support: that is, capacity can be defined as the sum volumetric concentration, c (sediment volume per unit volume, vol/vol), of all material in suspension at the net erosional-depositional threshold (Dorrell et al., 2013, and references therein). Competence describes the maximum particle size that can be transported by a flow. Although these two limits on particle transport are fundamentally related (Dorrell et al., 2013), most approaches to threshold calculation only incorporate one of these controls (e.g., Kubo et al., 2005, Shields, 1936), which reduces their effectiveness for general use.

2. Methods

Here we examine the ability of existing models to describe the erosion-deposition threshold of suspended load sediment transport by comparing them to a collated empirical data set of equilibrium flow (Ashida & Okabe, 1982; Brooks, 1954; Cellino & Graf, 1999; Coleman, 1986; Einstein & Chien, 1955; Graf & Cellino, 2002; Guy et al., 1966; Lyn, 1988; Nordin & Dempster, 1963; Vanoni, 1946; Vanoni & Nomicos, 1960). We then introduce a new sediment transport model that incorporates polydispersity and allows for both competence and capacity-driven sedimentation, and demonstrate that this outperforms existing models.

2.1. Empirical Data

The collated empirical data set includes flows with both narrow and wide particle size distributions and experimental and field observations (see Supporting Data Table S1). Collected data were restricted to flat beds to avoid enhanced sediment suspension effects arising from flow over an uneven bed (Soulsby, 1997).

As reported in original data sources, empirical measurements collated include depth average flow velocity, u, and shear velocity, u_*; flow depth, h; depth average concentration of the suspended load, c; and the particle size distribution at threshold conditions (see section 2.2). Original data sources use different models to determine shear velocity, that is, (i) depth-based, $u_* = \sqrt{ghS}$, where g is gravity and S is bed slope (Guy et al., 1966; Nordin & Dempster, 1963); (ii) hydraulic-radius based $u_* = \sqrt{gR_hS}$, where R_h is the hydraulic radius (Coleman, 1986; Einstein & Chien, 1955; Lyn, 1988; Vanoni, 1946; Vanoni & Nomicos, 1960); (iii) Reynolds-stress based, either derived from fitting a Rouse number to the flow's equilibrium concentration profile (Ashida & Okabe, 1982) or fitting the shear velocity to the shear stress profile (Cellino & Graf, 1999; Graf & Cellino, 2002); and (iv) bed-friction $u_* = u\sqrt{f_b/8}$, where f_b is a specified bed friction coefficient (Brooks, 1954). Depth average variables were calculated by integrating empirical profiles over the height of the flow and dividing by the flow depth.

2.2. Particle Size Distribution Fitting

To close both monodisperse and polydisperse models of the threshold between net erosional and depositional flow, both a characteristic suspended load particle size and the particle size distribution are determined from the collated empirical data (Figures 1 and 2). Monodisperse models are closed using the median particle size, d_{50}, although other authors have used different percentile particle sizes to characterize suspended and bedload sediment transport (van Rijn, 1984a).

The collated set of empirical data of flow at the threshold between net erosion and deposition can be separated into three types based on particle size data recorded (see Figure 1 and Supporting Data Table S1):

1. Both the initial (before use in laboratory experiments) and the suspended load size distribution are recorded (Experiments 1–7, from Guy et al., 1966).

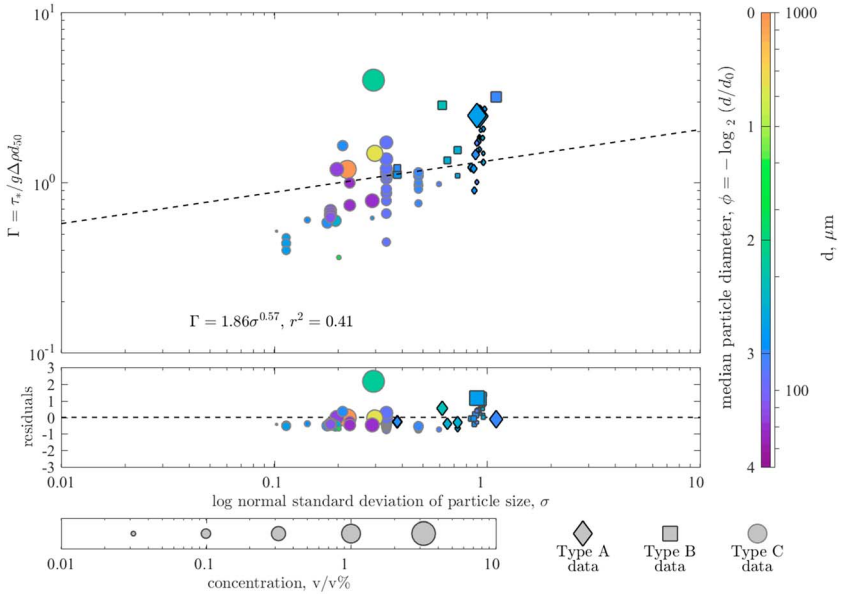

Figure 1. Dimensionless shear stress, Γ, at the net erosion-deposition threshold, as a function of lognormal standard deviation of the particle-size (see section 2.2). Residuals plot deviation from line of best fit. The colors denote ϕ-scale median particle size, where $\phi = -\log_2(d/d_0)$ and $d_0 = 1$ mm. Concentration is depicted by symbol size. Empirical data types (A–C), and original sources, are defined in section 2 and in Supporting Data Table S1.

2. Only the size distribution of the suspended load (fluvial data) is recorded (Experiments 8–30, from Nordin & Dempster, 1963).
3. Only the initial size distribution of material before use in laboratory experiments is recorded (Experiments 31–70, from Ashida & Okabe, 1982; Brooks, 1954; Coleman, 1986; Cellino & Graf, 1999; Einstein & Chien, 1955; Graf & Cellino, 2002; Lyn, 1988; Vanoni, 1946; and Vanoni & Nomicos, 1960).

The type A and B empirical data may be directly used to determine an appropriate particle size distribution. Here a skewed log-normal distribution, with a cumulative distribution function, *CDF*(ϕ),

$$\mathrm{CDF}(\phi) = \int_{-\infty}^{\phi}\left(\sqrt{\frac{2}{\omega^2\pi}}e^{-\frac{1}{2}\left(\frac{x-\xi}{\omega}\right)^2}\int_{-\infty}^{\psi\left(\frac{x-\xi}{\omega}\right)}e^{-\frac{t^2}{2}}dt\right)dx, \tag{1}$$

is fitted to empirical measurements of the CDF for three ϕ-scale particle sizes (fine, medium, and coarse). The distribution is discretized, using a ϕ-scale bin size of 0.01. The location, ξ; scale, ω; and shape, ψ, parameters are calculated by solving the resultant set of linked numerical equations using Matlab's nonlinear system solver, fsolve, based on Powell's method (Powell, 1964). The derived particle distribution is constrained to the central 99% region of a fitted probability function to avoid infinitely small and infinitely large particle classes.

For the type C data, a direct fit to particle size data cannot be used, as fractionation will result in change in the particle size distribution (Whitehouse, 1995). It is found from the type A data that the median particle size of suspended load, $\widetilde{\varphi}_{50}$ (as denoted by tilde notation), is consistently equivalent to the 8th percentile of the initial distribution, φ_{08}. This agrees with previous studies that report the median suspended load particle size as in the range of 2nd to 15th percentiles of material comprising the bed (Whitehouse, 1995). Although this fractionation rule may not hold for predominately fine-grained systems (see, e.g., Nittrouer, Mohrig, & Allison, 2011), the median size of the type A data ranges from $2.97 \geq \phi_{50} \geq 2.33$ and the median (unweighted) size of the type C data is also coarse, predominantly in the range $3 \geq \phi_{50} \geq 2$ (see Supporting Data Table S1). Thus, for the type C data, only the assumed suspended load distribution is weighted, following the empirical rule determined above, to account for particle fractionation. However, scale and shape parameters are assumed unchanged in the weighted distribution. A two-stage process is thus used to determine a characteristic particle size distribution:

1. A fit of a skewed log-normal distribution to initial particle data to determine: the 8th percentile particle size and the scale, ω, and shape, ψ, parameters.

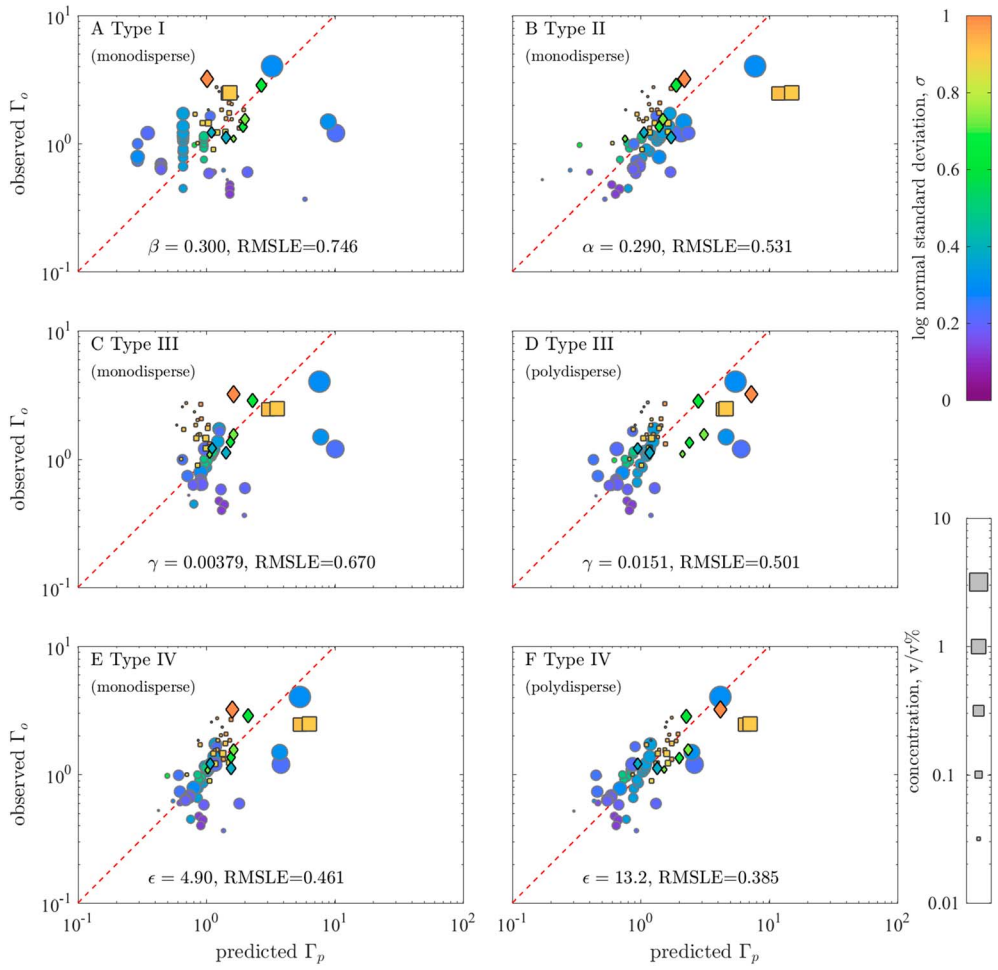

Figure 2. Comparison of empirical and modeled net erosion-deposition thresholds. Plots show the observed, Γ_o, versus the predicted, Γ_p, dimensionless shear stress for: monodisperse models Types (a) I, (b) II and (c) III and (e) IV, and the polydisperse models (d) III and (f) IV. Symbols are as in Figure 1, the dashed red line describes exact fit. The colors refer to the log-normal standard deviation of particle-size, σ.

2. A shift in the fitted skewed log-normal distribution such that $\widetilde{\varphi}_{50}$ is equivalent to φ_{08}.

The particle distribution shift in stage 2 is made using Matlab's fsolve to find a new weighted location parameter, $\widetilde{\xi}$, such that for the initial particle size distribution, the cumulative distribution function evaluated at, ϕ_{08}, is equal to 50%, that is, $\mathrm{CDF}\left(\phi_{08}, \widetilde{\xi}, \omega, \psi\right) = 50\%$.

3. Results

3.1. Particle-Laden Flow Hydrodynamics at Equilibrium

Here the hydrodynamics of particle-laden flow at equilibrium are quantified by the dimensionless ratio of the flow force acting on stationary particles to their submerged weight: here defined as $\Gamma = \tau_*/g\Delta\rho d_{50}$, where τ_*, $\Delta\rho = \rho_s - \rho$, and d_{50}, respectively, denote shear stress (characterized by a shear velocity: ${u_*}^2 = \tau_*/\rho$), particle-fluid density difference, and median particle diameter. The dimensional critical shear velocity for incipient particle motion of a particulate bed is denoted u_{*_c}. Such an approach is chosen as it allows direct comparison to the common dimensionless models of incipient motion (Shields, 1936) and the Rouse condition for suspended load transport (Rouse, 1937). Examination of the collated laboratory and field data set of flows at the net erosional-depositional threshold shows that the hydrodynamics of the particle-laden flow at equilibrium are intrinsically related to the particle size distribution. The dimensionless shear stress required to maintain threshold conditions increases as the particle size distribution widens (Figure 1). This

effect even occurs when the median particle size remains constant and thus cannot be captured by monodisperse models.

3.2. Net Erosion and Deposition Threshold Models

Existing models of the net erosional-depositional threshold are tested and compared against empirical observations. The goodness of fit between observed, Γ_o, and predicted, Γ_p, dimensionless shear stress (Figure 2), is given by the Root Mean Square Logarithmic Error (RMSLE) for which smaller numbers represent lower error. A new model is then proposed based on these comparisons.

3.2.1. Rouse Models

In competence-based (Type I "Rouse") models, deposition rate is an assumed function of flow stratification. As stratification scales with the settling to shear velocity ratio (Soulsby, 1997), some equilibrium flow models (Kneller, 2003; Komar, 1985; Kubo et al., 2005; Lynds et al., 2014) have assumed a net erosional-depositional threshold given by

$$w_s = \beta u_*, \tag{2}$$

where w_s is the (particle-size dependent) characteristic particle settling velocity (see the supporting information) and β is an empirical Rouse parameter (Rouse, 1937). Settling velocity is estimated based on the median particle diameter. Although alternative models have used different percentile particle sizes to characterize the settling velocity of sediment in suspension, they may all be criticized as failing to describe the dynamics of the finer or coarser particle classes, respectively (see Komar, 1985, and references therein). An iterative best fit of the theoretical model to data yields $\beta = 0.300$ and RMLSE = 0.746 (Figure 2a). The Rouse parameter describes a threshold between erosion and deposition independent of concentration or particle size distribution. Regardless of whether the particle size distribution can be ignored, the Rouse criterion must be fundamentally flawed as the threshold condition is known to be dependent on the concentration of material in suspension (Garcia, 2008). A corollary is that the commonly used transition criterion between bedload (transport dominated by particle-bed interaction) and suspended load (transport dominated by turbulent fluid motion), $u_* = w_s$ (Soulsby, 1997) should also take concentration into account (see the supporting information).

3.2.2. Flow Power Models

Capacity-based (Type II "Flow Power") models assume that when deposition and erosion are in balance, the rate of work done keeping material in suspension, $g\Delta\rho c w_s$, is directly proportional to available flow power (Bagnold, 1966; Celik & Rodi, 1991; Garcia, 2008; Velikanov, 1954), that is proportional to $\rho u_*^3/h$ (see the supporting information; Pope, 2000; Wright & Parker, 2004). The net erosional-depositional threshold is thus implicitly defined by

$$g\Delta\rho c w_s h = \alpha\rho u_*^3. \tag{3}$$

In equation (3) h is flow depth and α is an empirical constant specifying the energy efficiency of the flow (Bizzi & Lerner, 2015; Li et al., 2014). An iterative best fit of the theoretical model to data yields $\alpha = 0.290$ and RMLSE = 0.531 (Figure 2b). Although derivable from first principles (see the supporting information), mechanistic flow power models do not offer a means to account for particle size distribution or competence effects on threshold conditions.

3.2.3. Flux Balance Models

Alternatively, competence-capacity-based (Type III "Flux Balance") models equate the net rate of sediment entrainment from the bed to the net rate of deposition from suspended load (Garcia, 2008; Garcia & Parker, 1991, 1993; Smith & Hopkins, 1973), a formulation that can be traced back to the original morphodynamic models of Exner (1920, 1925). For a polydisperse suspension of N distinct particle classes, individual, c_i, and sum, $c = \sum_{i=1}^{N} c_i$, particle class concentrations determine the criteria for threshold flow (Dorrell et al., 2013), as given by the $N + 1$ conditions

$$\frac{c_i^-}{c_m} E_i = c_i^+ w_{si} \forall i \text{ and } \sum_{i=1}^{N} c_i^- = c_m. \tag{4}$$

Here the sediment entrainment rate is defined by E_i; the packing concentration, $c_m = 0.6$, is assumed constant (Dorrell & Hogg, 2010); particle class concentration near the bed, at height $z^+ = 0.01$ h (Soulsby, 1997), is defined by c_i^+; and particle class concentration in the active layer of the bed, which freely exchanges

material with material transported as suspended load (Dorrell et al., 2013), is defined by c_i^-. Here particle distribution-dependent hiding effects in the active layer are assumed negligible (Wilcock & Southard, 1988) and the active layer is assumed to contain only particle classes also in suspension (Dorrell et al., 2013). Given the near-bed concentration and sediment entrainment rate, the threshold condition is given by the minimum shear velocity that satisfies equation (4) where $0 \leq c_i^- \leq c_m$. Near bed concentration is proportional to individual capacity $c_i^+ = c_i/\lambda_i$; assuming that the flow is dilute and turbulence dampening is negligible (see, e.g., Gelfenbaum & Smith, 1986; Smith & McLean, 1977; van Rijn, 1984a), the shear and particle settling velocity-dependent stratification shape function, λ_i, is given by the depth-averaged Rouse profile (see the supporting information; Rouse, 1937).

Previous studies suggest that entrainment rate is a competence-limited function of forces applied to the bed, that is, the available flow power above that required for incipient particle motion given by $\Delta u_{*i}^3/h = \max(u^{*2} - u_{*ci}^2, 0)^{3/2}/h$ (van Rijn, 1984b) and the properties of the material being entrained (van Rijn, 1984b; Garcia & Parker, 1991, 1993), that is, particle size, d_i. Here u_{*ci} is the critical shear velocity for incipient motion of a particle of given size. To close equation (4), a common sediment entrainment function, based on erosional flow experiments (Basani et al., 2014; Dorrell et al., 2013; van Rijn, 1984b), is used that takes the form

$$E_i = \gamma\rho(g\Delta\rho d_i)^{-1}\Delta u_{*i}^3 \tag{5}$$

(γ being an empirical parameter describing entrainment efficiency). This particle-size dependent entrainment function is employed in current (Type III) models, equations (4) and (5). An iterative best fit of the monodisperse form of this model to data yields $\gamma = 3.79 \times 10^{-3}$ and a RMSLE = 0.670 (Figure 2c). Using a polydisperse model to explicitly model size distribution improves the fit giving $\gamma = 1.51 \times 10^{-2}$ and a RMSLE = 0.501 (Figure 2d).

3.2.4. Flow-Power Flux-Balance Model

In the limit of a monodisperse unstratified suspension, where deposition scales with cw_s (Dorrell et al., 2013), the flow power model (3) implies that erosion of sediment scales with $\rho u_*^3/g\Delta\rho h$. However, the flux balance model, equations (4) and (5), does not recover this mechanistic description of the flow. In the regime of an unstratified suspension, $w_s \ll u_*$, a series expansion of the flux balance model (equations (4) and (5)) implies that equilibrium erosion (in balance with deposition) scales inversely with particle diameter, $cw_s \propto \rho u_*^3/(g\Delta\rho d)$, to leading order.

This result motivates the development of a new flow-power, flux-balance (Type IV) model that recovers the mechanistic flow power model $cw_s \propto \rho u_*^3/(g\Delta\rho h)$ of threshold flow, for $w_s \ll u_*$; describes flow competence; and may be extended to describe polydisperse suspensions. This is achieved using a new sediment entrainment function for flow at the threshold between net erosion and net deposition. Here the power required to lift sediment into suspended load, $g\Delta\rho E_i$, is assumed proportional to the depth-averaged available flow power, $\rho\Delta u_{*i}^3/h$. While entrainment is limited by particle-size dependent competence, the new entrainment function has the form

$$E_i = \varepsilon\rho(g\Delta\rho h)^{-1}\Delta u_{*i}^3, \tag{6}$$

which scales with flow depth and is a key departure from existing entrainment models that are scaled using particle diameter (ε being an empirical parameter describing entrainment efficiency). This flow depth-dependent entrainment function is used to close the flow-power flux-balance (Type IV) model, equations (4) and (6), An iterative best fit of the monodisperse form of this model to empirical data yields $\varepsilon = 4.90$ and a RMSLE = 0.461 (Figure 2c); the polydisperse form of this model improves the fit, where $\varepsilon = 13.2$ and a RMSLE = 0.385 (Figure 2d). The improvement in threshold flow predictions by using a flow depth rather than particle diameter (Garcia & Parker, 1993; van Rijn, 1984b) scaled entrainment rate is also demonstrated by the decrease in RMSLE from 0.501 to 0.385 between the Type III and IV models (Figures 2d and 2f).

3.3. Reference Concentration

A reference concentration condition is often used to close modeled sediment in suspension (Soulsby, 1997). As stressed by Dorrell and Hogg (2011), such a boundary condition can only be applied at the threshold between net erosion and deposition, as its use in temporally or spatially evolving flows may result in

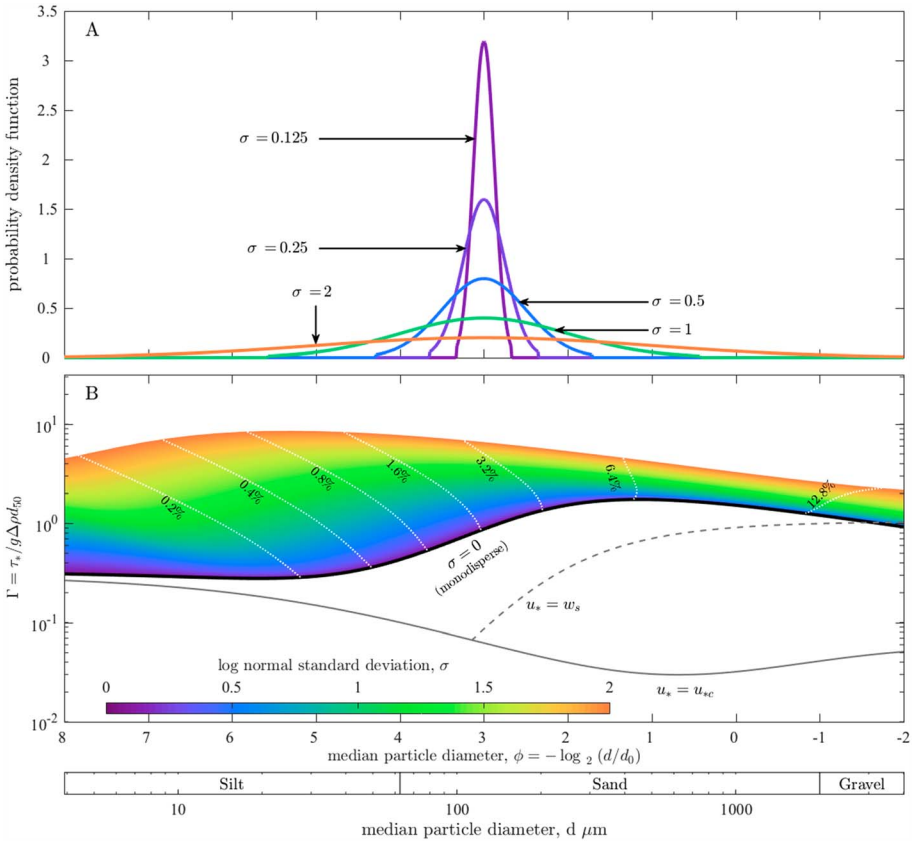

Figure 3. Dependence of the dimensionless shear stress, Γ, on particle size standard deviation. (a) Lognormal suspended load particle size distributions, truncated to the central 99% range. (b) Threshold dimensionless shear stress, Γ, derived using the flux balance model (Type IV), at average empirical flow conditions (c = 0.1% and h = 0.25 m; see Supporting Data Table S1). Particle size distribution is specified a priori by a log-normal distribution (a). The dotted white curves describe the near-bed reference concentration, $\Sigma_{i=1}^{N} c_i^+$. The solid gray curve denotes the Shields condition for incipient motion, while the dashed gray curve denotes the Rouse condition for suspended load transport.

erroneous gravitationally unstable profiles of suspended sediment concentration. The reference concentration may easily be determined from the flux balance models (Type III and IV) as the sum near-bed concentration, $\sum_{i=1}^{N} c_i^+$; see Figure 3. For example, assuming the capacity to transport particles in suspension is indeed related to flow power (Bagnold, 1966; Velikanov, 1954), the near-bed reference concentration is shown from equations (4) and (6) to be a function of the composition of the active layer of the bed and particle size (settling velocity) distribution

$$\sum_{i=1}^{N} c_i^+ = \sum_{i=1}^{N} \varepsilon \frac{\rho}{(g\Delta\rho h)} \frac{c_i^-}{c_m} \frac{\Delta u_{*i}^3}{w_{si}} \quad \text{where} \sum_{i=1}^{N} c_i^- = c_m. \tag{7}$$

Therefore, the near-bed suspended load reference concentration must be particle size (settling velocity)-dependent, given the balance between the work done keeping sediment in suspension and the available power of the flow. This contrasts with research that hypothesizes that near-bed concentration is particle-size independent (for particles <200 μm in diameter) (e.g., Eggenhuisen et al., 2017). More generally, the reference concentration is also dependent on the composition of the active layer, c_i^-. Thus, there is no unique solution for the suspended load capacity of a polydisperse suspension of particulate material at a given shear velocity (Dorrell et al., 2013). However, if the concentration, size distribution, and the shear velocity dependence of the vertical distribution of material in suspension are known, a unique solution for the shear velocity at the threshold between net deposition and erosion may be found using the flux balance models, Types III and IV (Figures 2 and 3).

4. Discussion

Comparing all the models discussed, monodisperse models in general provide a poorer collapse between the observed, Γ_o, and predicted, Γ_p, dimensionless shear (Figures 2a–2c). The discretization of particle size distribution improves model predictions; the polydisperse form of the new Type IV model, which uses the flow power based sediment entrainment formula, provides the best collapse (Figure 2f). Notably, where suspended particle size distribution was explicitly recorded (i.e., the 30 experiments comprising the type A and B data), the Type IV model provides the best prediction of threshold between net erosion-deposition (compare Figures 2b and 2f). Fit of the type C data is also improved using the Type IV model, but this depends on the interpolated distribution of material in suspension (section 2.2). Moreover, discretization of the particle size distribution significantly improves prediction of flow conditions recorded in laboratory and fluvial observations (compare Figures 2e and 2f). This is due to increasingly wider particle size distributions enhancing vertical flow stratification and thus depositional flux. Consequently, the shear stress must increase for the flow to maintain the net erosional-depositional threshold. The effect of stratification is magnified by the nonlinear dependence of settling velocity on particle size (Soulsby, 1997).

As shown in Figure 3, the net erosion-deposition threshold for particulate laden flows at equilibrium occurs in the suspended load regime. In contrast to previous studies, where sediment transport was predicted using characteristic particle size (see, e.g., Bagnold, 1966; Bizzi & Lerner, 2015; Celik & Rodi, 1991; Kubo et al., 2005; Soulsby, 1997; Velikanov, 1954; Yang, 2006), the net erosion-deposition threshold is shown to also depend strongly on particle size distribution (Figures 1 and 3). For example, the dimensionless shear stress required to maintain threshold conditions for coarse silt ($\varphi = 5$) increases by ~3,000% when varying from monodisperse, $\sigma = 0$, to poorly sorted (Folk, 1966), $\sigma \approx 2$, sediment (Figure 3b). In contrast, changes in characteristic particle size have a comparatively small effect, with a maximum ~250% increase in dimensionless shear stress for $8 \geq \varphi \geq -2$ and $\sigma = 1$ (Figure 3b). Thus, particle size distribution is a dominant control on the dimensionless shear stress at the threshold between net erosional and depositional flow; although, it is noted, from Figure 1, that characteristic particle size and suspended load concentration also affect this threshold. Moreover, this threshold also influences other critical sediment transport parameters including flow concentration (i.e., capacity) and in turn the maximum sediment transport flux per unit area (i.e., the product of flow concentration and velocity, which is proportional to shear stress). The order of magnitude variations in dimensionless shear stress with particle size distribution (Figure 3) may thus explain the large errors inherent in existing monodisperse sediment transport models (Yang, 2006).

As posed, sediment concentration, determined by stratification (2), flow power (3), or entrainment, equations (5) and (6), increases with the amount of turbulent mixing characterized by shear velocity. However, with increasing volume concentration, there is a nonlinear relationship between the energy needed to keep material in suspension and flow power, since turbulence is progressively dampened with suspension of particulate material (Yang, 2006). Thus, the threshold formulation, equations (2)–(6), only holds for dilute flow, not for the sub-super saturated threshold of hyperconcentrated flows (van Maren et al., 2009). Transition to hyperconcentrated flow occurs across a wide range of concentrations, $0.1 < c < 0.4$ (see van Maren et al., 2009, and references therein). Moreover, while we have proposed empirical closures scaling the dependence on shear velocity, further work is required to elucidate the physical processes controlling these scaling parameters.

Here we have shown that the effect of particle size distribution on controlling the threshold between net erosion and net deposition from suspended load transport is far more important than has previously been recognized. Previous work may have overstated the predictive ability of monodisperse models as they have predominantly compared them to comparatively narrow particle size distributions. Comparison to wider particle size distributions, typical of many natural environments and industrial settings, demonstrates the limitations of these monodisperse models and the importance of particle size distribution (Figure 3).

5. Conclusions

Here it is shown that particle size distribution is a dominant control on the threshold between net erosion and net deposition of suspended particles in environmental and industrial flows. Thus, polydisperse, rather than monodisperse, particle size modeling approaches are required to predict the threshold between the entrainment and deposition of particulate material into suspended load. Broader particle size distributions enhance suspended sediment stratification and thus the near-bed sediment concentration and depositional flux.

Consequently, threshold conditions occur at higher shear stresses in flows carrying broader particle distributions compared with those carrying narrower distributions. Therefore, the threshold does not have unique values for specific combinations of flow concentration and characteristic particle size—implicit in existing theories—but has a range of possible values depending on particle size distribution. To predict the threshold, a new sediment entrainment function is proposed based on the flow-power model of suspended load particle transport capacity. By doing so, suspended load polydispersity is incorporated, providing a better than order-of-magnitude improvement compared to existing models. The results also explain the wide variations observed in current models when the net erosional-depositional threshold is based on a characteristic particle size. This model establishes a basis for accurate predictions of particle-laden flow hydrodynamics and morphodynamics, applicable across a wide range of environmental, engineering, and industrial settings.

Acknowledgments
This work was supported by the Turbidites Research Group, University of Leeds, UK. We thank Alan Haywood, Jim Hendy, Nigel Mountney, and Paul Wignall for helpful discussions and commenting on the initial manuscript. We thank David Mohrig and Joris Eggenhuisen for providing thought provoking reviews that have significantly improved the paper. Data used are detailed in the supporting information.

References

Armanini, A., & Di Silvio, G. (1988). A one-dimensional model for the transport of a sediment mixture in non-equilibrium conditions. *Journal of Hydraulic Research*, *26*(3), 275–292. https://doi.org/10.1080/00221688809499212

Ashida, K., & Okabe, T. (1982). On the calculation method of the concentration of suspended sediment under non-equilibrium condition. In *Proceedings of the 26th conference on hydraulics* (pp. 153–158.

Bagnold, R. A. (1966). *An approach to the sediment transport problem* (Vol. 442-I). Washington, DC: Geological Survey Professional Paper.

Basani, R., Janocko, M., Cartigny, M. J., Hansen, E. W., & Eggenhuisen, J. T. (2014). MassFLOW-3DTM as a simulation tool for turbidity currents?: Some preliminary results. In A. W. Martinius, et al. (Eds.), *In Depositional systems to sedimentary successions on the norwegian continental margin*, *International Association of Sedimentologists. Special Publication* (Vol. 46, pp. 587–608).

Bayat, H., Rastgo, M., Zadeh, M. M., & Vereecken, H. (2015). Particle size distribution models, their characteristics and fitting capability. *Journal of Hydrology*, *529*, 872–889. https://doi.org/10.1016/j.jhydrol.2015.08.067

Bizzi, S., & Lerner, D. N. (2015). The use of stream power as an indicator of channel sensitivity to erosion and deposition processes. *River Research and Applications*, *31*(1), 16–27. https://doi.org/10.1002/rra.2717

Blom, A., & Parker, G. (2004). Vertical sorting and the morphodynamics of bed form–dominated rivers: A modeling framework. *Journal of Geophysical Research*, *109*, F02007. https://doi.org/10.1029/2003JF000069

Brooks, N. H. (1954). Laboratory studies of the mechanics of streams flowing over a movable bed of fine sand, (Doctoral dissertation) California Institute of Technology.

Bufe, A., Paola, C., & Burbank, D. W. (2016). Fluvial bevelling of topography controlled by lateral channel mobility and uplift rate. *Nature Geoscience*, *9*(9), 706–710. https://doi.org/10.1038/ngeo2773

Celik, I., & Rodi, W. (1991). Suspended sediment-transport capacity for open channel flow. *Journal of Hydraulic Engineering*, *117*(2), 191–204. https://doi.org/10.1061/(ASCE)0733-9429(1991)117:2(191)

Cellino, M., & Graf, W. H. (1999). Sediment-laden flow in open-channels under noncapacity and capacity conditions. *Journal of Hydraulic Engineering*, *125*(5), 455–462. https://doi.org/10.1061/(ASCE)0733-9429(1999)125:5(455)

Coleman, N. L. (1986). Effects of suspended sediment on the open-channel velocity distribution. *Water Resources Research*, *22*(10), 1377–1384. https://doi.org/10.1029/WR022i010p01377

Dorrell, R., & Hogg, A. J. (2010). Sedimentation of bidisperse suspensions. *International Journal of Multiphase Flow*, *36*, 481–490. https://doi.org/10.1016/j.ijmultiphaseflow.2010.02.001

Dorrell, R. M., & Hogg, A. J. (2011). Length and time scales of response of sediment suspensions to changing flow conditions. *Journal of Hydraulic Engineering*, *138*, 430–439.

Dorrell, R. M., Hogg, A. J., & Pritchard, D. (2013). Polydisperse suspensions: Erosion, deposition, and flow capacity. *Journal of Geophysical Research: Earth Surface*, *118*, 1939–1955. https://doi.org/10.1002/jgrf.20129

Eggenhuisen, J. T., Cartigny, M. J., & de Leeuw, J. (2017). Physical theory for near-bed turbulent particle suspension capacity. *Earth Surface Dynamics*, *5*(2), 269–281. https://doi.org/10.5194/esurf-5-269-2017

Einstein, H. A., & Chien, N. (1955). Effects of heavy sediment concentration near the bed on velocity and sediment distribution. Missouri River Division, Corps of Engineers, US Army.

Exner, F. M. (1920). Zur physik der dünen. Hölder.

Exner, F. M. (1925). Uber die wechselwirkung zwischen wasser und geschiebe in flussen. *Akademie der Wissenschaften in Wien. Mathematisch-Naturwissenschaftliche Klasse*, *134*, 165–204.

Folk, R. L. (1966). A review of grain-size parameters. *Sedimentology*, *6*(2), 73–93. https://doi.org/10.1111/j.1365-3091.1966.tb01572.x

Garcia, M. H. (2008). Sediment transport and morphodynamics. In M. H. Garcia (Ed.), *Sedimentation engineering: Processes, measurements, modeling and practice. ASCE manuals and reports on engineering practice No. 110* (pp. 21–164). Reston, VA: American Society of Civil Engineers. https://doi.org/10.1061/9780784408148.ch02

Garcia, M. H., & Parker, G. (1991). Entrainment of bed sediment into suspension. *Journal of Hydraulic Engineering*, *117*(4), 414–435. https://doi.org/10.1061/(ASCE)0733-9429(1991)117:4(414)

Garcia, M. H., & Parker, G. (1993). Experiments on the entrainment of sediment into suspension by a dense bottom current. *Journal of Geophysical Research*, *98*(C3), 4793–4807. https://doi.org/10.1029/92JC02404

Gelfenbaum, G., & Smith, J. D. (1986). Experimental evaluation of a generalized suspended-sediment transport theory. In R. J. Knight & S. R. McLean (Eds.), *Shelf sands and sandstones, Canadian Society of Petrolium Geologists* (pp. 133–144). Calgary, Alberta.

Graf, W. H., & Cellino, M. (2002). Suspension flows in open channels; experimental study. *Journal of Hydraulic Research*, *40*(4), 435–447. https://doi.org/10.1080/00221680209499886

Guy, H. P., Simons, D. B., & Richardson, E. V. (1966). Summary of alluvial channel data from flume experiments, 1956-61. US Geological Survey Professional Paper 462-I.

Halsey, T. C., Kumar, A., & Perillo, M. M. (2017). Sedimentological regimes for turbidity currents: Depth-averaged theory. *Journal of Geophysical Research: Oceans*, *122*, 5260–5285. https://doi.org/10.1002/2016JC012635

Houssais, M., Ortiz, C. P., Durian, D. J., & Jerolmack, D. J. (2015). Onset of sediment transport is a continuous transition driven by fluid shear and granular creep. *Nature Communications*, *6*, 1–8.

Kneller, B. (2003). The influence of flow parameters on turbidite slope channel architecture. *Marine and Petroleum Geology*, *20*(6-8), 901–910. https://doi.org/10.1016/j.marpetgeo.2003.03.001

Komar, P. D. (1985). The hydraulic interpretation of turbidites from their grain sizes and sedimentary structures. *Sedimentology*, *32*(3), 395–407. https://doi.org/10.1111/j.1365-3091.1985.tb00519.x

Kubo, Y. S., Syvitski, J. P., Hutton, E. W., & Paola, C. (2005). Advance and application of the stratigraphic simulation model 2D-SedFlux: From tank experiment to geological scale simulation. *Sedimentary Geology*, *178*(3-4), 187–195. https://doi.org/10.1016/j.sedgeo.2005.04.005

Li, W., van Maren, D. S., Wang, Z. B., de Vriend, H. J., & Wu, B. (2014). Peak discharge increase in hyperconcentrated floods. *Advances in Water Resources*, *67*, 65–77. https://doi.org/10.1016/j.advwatres.2014.02.007

Lyn, D. A. (1988). A similarity approach to turbulent sediment-laden flows in open channels. *Journal of Fluid Mechanics*, *193*(1), 1–26. https://doi.org/10.1017/S0022112088002034

Lynds, R. M., Mohrig, D., Hajek, E. A., & Heller, P. L. (2014). Paleoslope reconstruction in sandy suspended-load dominated rivers. *Journal of Sedimentary Research*, *84*(10), 825–836. https://doi.org/10.2110/jsr.2014.60

McLean, S. R. (1991). Depth-integrated suspended-load calculations. *Journal of Hydraulic Engineering*, *117*(11), 1440–1458. https://doi.org/10.1061/(ASCE)0733-9429(1991)117:11(1440)

McLean, S. R. (1992). On the calculation of suspended load for noncohesive sediments. *Journal of Geophysical Research*, *97*(C4), 5759–5770. https://doi.org/10.1029/91JC02933

Nittrouer, J. A., Best, J. L., Brantley, C., Cash, R. W., Czapiga, M., Kumar, P., & Parker, G. (2012). Mitigating land loss in coastal Louisiana by controlled diversion of Mississippi River sand. *Nature Geoscience*, *5*, 534–537. https://doi.org/10.1038/ngeo1525

Nittrouer, J. A., Mohrig, D., & Allison, M. (2011). Punctuated sand transport in the lowermost Mississippi River. *Journal of Geophysical Research*, *116*, F04025. https://doi.org/10.1029/2011JF002026

Nordin, C. F., & Dempster, G. R. (1963). Vertical distribution of velocity and suspended sediment, Middle Rio Grande, New Mexico, US Geological Survey Professional Paper 462-B.

Parsi, M., Najmi, K., Najafifard, F., Hassani, S., McLaury, B. S., & Shirazia, S. A. (2014). A comprehensive review of solid particle erosion modeling for oil and gas wells and pipelines applications. *Journal of Natural Gas Science and Engineering*, *21*, 850–873. https://doi.org/10.1016/j.jngse.2014.10.001

Pope, S. B. (2000). *Turbulent Flows*. Cambridge, UK: Cambridge University Press. https://doi.org/10.1017/CBO9780511840531

Powell, M. J. D. (1964). An efficient method for finding the minimum of a function of several variables without calculating derivatives. *The Computer Journal*, *7*(2), 155–162. https://doi.org/10.1093/comjnl/7.2.155

Rouse, H. (1937). Modern conceptions of the mechanics or fluid turbulence. *Transactions of the American Society of Civil Engineers*, *102*, 463–505.

Sajeesh, P., & Sen, A. K. (2014). Particle separation and sorting in microfluidic devices: A review. *Microfluidics and Nanofluidics*, *17*(1), 1–52. https://doi.org/10.1007/s10404-013-1291-9

Shields, A. (1936). *Anwendung der Aehnlichkeitsmechanik und der Turbulenzforschung auf die Geschiebebewegung*. Berlin: Preussischen Versuchsanstalt für Wasserbau.

Smith, J. D., & Hopkins, T. S. (1973). Sediment transport on the continental shelf off of Washington and Oregon in light of recent current measurements. In D. J. P. Swift, D. B. Duane, & O. H. Pilkey (Eds.), *Shelf sediment transport: Process and patterns* (pp. 143–179). Stroudsburg, PA: Hutchinson and Ross.

Smith, J. D., & McLean, S. R. (1977). Spatially averaged flow over a wavy surface. *Journal of Geophysical Research*, *82*(12), 1735–1746. https://doi.org/10.1029/JC082i012p01735

Soulsby, R. (1997). *Dynamics of marine sands: A manual for practical applications*. UK: Thomas Telford Publications.

Strauss, M., & Glinsky, M. E. (2012). Turbidity current flow over an erodible obstacle and phases of sediment wave generation. *Journal of Geophysical Research*, *117*, C06007. https://doi.org/10.1029/2011JC007539

Syvitski, J. P., Peckham, S. D., Hilberman, R., & Mulder, T. (2003). Predicting the terrestrial flux of sediment to the global ocean: A planetary perspective. *Sedimentary Geology*, *162*(1-2), 5–24. https://doi.org/10.1016/S0037-0738(03)00232-X

van Maren, D. S., Winterwerp, J. C., Wang, Z. Y., & Pu, Q. (2009). Suspended sediment dynamics and morphodynamics in the Yellow River, China. *Sedimentology*, *56*, 785–806. https://doi.org/10.1111/j.1365-3091.2008.00997.x

van Rijn, L. C. (1984a). Sediment transport, part II: Suspended load transport. *Journal of Hydraulic Engineering*, *110*(11), 1613–1641. https://doi.org/10.1061/(ASCE)0733-9429(1984)110:11(1613)

van Rijn, L. C. (1984b). Sediment pick-up functions. *Journal of Hydraulic Engineering*, *110*(10), 1494–1502. https://doi.org/10.1061/(ASCE)0733-9429(1984)110:10(1494)

Vanoni, V. A. (1946). Transportation of suspended sediment by water. *Transactions of the American Society of Civil Engineers*, *111*, 67–102.

Vanoni, V. A., & Nomicos, G. N. (1960). Resistance properties of sediment-laden streams. *Transactions of the American Society of Civil Engineers*, *125*, 1140–1167.

Velikanov, M. A. (1954). Gravitational theory of sediment transport. *Journal of Science of the Soviet Union, Geophysics*, *4*.

Walling, D. E. (2009). The Impact of Global Change on Erosion and Sediment Transport by Rivers: Current Progress and Future Challenges. UNESCO, Paris.

Wang, S., Wang, S., Fu, B., Piao, S., Lü, Y., Ciais, P., et al. (2015). Reduced sediment transport in the Yellow River due to anthropogenic changes. *Nature Geoscience*, *9*, 38–42.

Whitehouse, R. (1995). Observations of the boundary layer characteristics and the suspension of sand at a tidal site. *Continental Shelf Research*, *15*(13), 1549–1567. https://doi.org/10.1016/0278-4343(95)00038-3

Wilcock, P. R., & Southard, J. B. (1988). Experimental study of incipient motion in mixed-size sediment. *Water Resources Research*, *24*(7), 1137–1151. https://doi.org/10.1029/WR024i007p01137

Wright, S., & Parker, G. (2004). Flow resistance and suspended load in sand-bed rivers: Simplified stratification model. *Journal of Hydraulic Engineering*, *130*, 796–805. https://doi.org/10.1061/(ASCE)0733-9429(2004)130:8(796)

Yang, C. T. (2006). *Erosion and Sedimentation Manual*. Denver, CO: US Department of the Interior, Bureau of Reclamation.